Available online at www.sciencedirect.com
ScienceDirect
Journal of the European Ceramic Society 27 (2007) 3161–3170
www.elsevier.com/locate/jeurceramsoc

Characteristics of ZnO-based varistor ceramics doped with Al_2O_3

S. Bernik *, N. Daneu

Jožef Stefan Insitute, Jamova 39, 1000 Ljubljana, Slovenia

Received 28 June 2006; received in revised form 24 January 2007; accepted 27 January 2007
Available online 30 March 2007

Abstract

The influence of Al_2O_3 doping in the range 0.00–0.83 mol% on the microstructure and current–voltage characteristics of ZnO-based varistor ceramics sintered at 1200 °C for 2 h was studied. The threshold voltage V_T (V/mm) increased up to a dopant level of about 0.08 mol% Al_2O_3; the nonlinear coefficient α was significantly increased by additions of up to 0.04 mol% Al_2O_3, although larger additions of Al_2O_3 caused it to decrease; and the leakage current increased sharply with increasing amounts of Al_2O_3. Doping with Al_2O_3 up to about 0.12 mol% Al_2O_3 resulted in a significantly decreased ZnO grain size, which is mainly responsible for the significantly increased threshold voltage, V_T. No $ZnAl_2O_4$ spinel phase was detected in any of the samples, and EDXS and WDXS analyses showed that most of the added Al_2O_3 distributed between the $Zn_7Sb_2O_{12}$ spinel phase and the ZnO phase, while only trace amounts were detected in the Bi_2O_3-rich phase. The spinel phase incorporates an appropriate amount of Al_2O_3; however, with an increasing amount of added Al_2O_3, more of it remains outside the spinel phase in the Bi_2O_3-rich liquid, where it can incorporate into the growing ZnO grains at the sintering temperature. The amount of Al in the ZnO grains was determined. A mechanism for the grain growth inhibition resulting from the small amounts of Al_2O_3 in the Bi_2O_3-rich liquid phase is also proposed.
© 2007 Elsevier Ltd. All rights reserved.

Keywords: Grain growth; Microstructure-final; Electrical properties; ZnO; Varistors

1. Introduction

ZnO-based ceramics doped with only a few mol% of oxides of Bi, Sb, Co, Mn, Ni, Cr and others – known as varistor ceramics – possess exceptional nonlinearity in their current–voltage characteristics and the ability to absorb large amounts of energy. For this reason varistors have been extensively used for the protection of electronic circuits, devices and equipment against voltage surges, and for the voltage stabilization of electrical power lines, for almost 30 years. The characteristics of varistor ceramics are closely related to their microstructure, which is characterized by the following: the ZnO grain size and the grain size distribution; the grain boundaries; secondary phases such as the Bi_2O_3-rich phase and the $Zn_7Sb_2O_{12}$ spinel-type phase (and the $Bi_3Zn_2Sb_3O_{14}$ pyrochlore-type phase can be present as well); the distribution of secondary phases along the grain boundaries; and the presence of porosity. Each of the dopants plays a distinctive role in the subtle tuning of the final nonlinear characteristics of the varistor ceramics and cannot be omitted. Also, the proper ratios among the dopants have to be set in order to obtain the required electrical performance of the varistor ceramics through the process of microstructure development.[1–3] Although the overall electrical characteristics of varistor ceramics result from the collective effect of all the microstructural features, two of them have key roles: (i) the grain boundaries between the ZnO grains, which have nonlinear current–voltage characteristics with an optimum break-down voltage of about 3V – unfortunately, it can be lower as well, or the grain boundary may not exhibit varistor behavior at all and possess ohmic characteristics – and define the characteristics of the varistor in the pre-break-down region, and (ii) the ZnO grains, which with their size define the number of grain boundaries between the electrodes and hence the break-down voltage of the varistor, and with their conductivity define the performance of the varistor at high currents in the upturn region of the current–voltage characteristic. Some dopants have a significant effect on the pre-break-down and the upturn current–voltage characteristics of varistors even when much lower amounts of additives than standard are added to the varistor. In very small amounts aluminum is a potential dopant for increasing the conductivity of the ZnO grains and enhancing the varistor's performance at high currents.[4–7] The doping behaviors of Al as well as some other

* Corresponding author. Tel.: +386 1 477 3682; fax: +386 1 426 3126.
E-mail address: slavko.bernik@ijs.si (S. Bernik).

0955-2219/$ – see front matter © 2007 Elsevier Ltd. All rights reserved.
doi:10.1016/j.jeurceramsoc.2007.02.176

minor dopants and their influence on the current–voltage characteristics of ZnO were thoroughly investigated and reported by Gupta.[8] Aluminum incorporates into the ZnO grains and influences the equilibrium of the crystal lattice defects. Depending on the concentration and the site of its incorporation into the ZnO lattice – regular Zn sites or interstitial sites – it can act either as a donor or an acceptor, or both, which defines its influence on the conductivity of the ZnO grains and also the characteristics of the grain boundaries: (i) as a donor it increases the conductivity of the ZnO grains and improves the varistor behavior at high currents, but it also results in an increased leakage current of the varistor in the pre-break-down region; (ii) as an acceptor it reduces the leakage current of the varistor, but it also reduces the conductivity of the ZnO grains, which has a negative effect on the varistor response to high currents and hence its energy characteristics. Other reports also confirmed that the effect of Al is very sensitive to the amount added to the varistor and also to the heat-treatment regime, i.e., the sintering temperature and time, and the cooling rate.[9,10] At lower concentrations of Al, up to a few thousand ppm, it is mainly the donor effect that is observed, while at higher concentrations, above 10,000 ppm, the acceptor effect prevails.[4,8] Doping with Al_2O_3 influences the grain growth of ZnO even for amounts as small as several tens of ppm added to the varistor composition.[4,8,11] The inhibition of ZnO grain growth by Al_2O_3 doping in varistor ceramics at low levels of doping is not explained yet, while at higher levels of doping, i.e., several thousands of ppm, in the binary ZnO-Al_2O_3 system or the ternary ZnO-Bi_2O_3-Al_2O_3 system the inhibition is attributed to the decreased mobility of the grain boundaries due to the $ZnAl_2O_4$ spinel phase that forms at the grain boundaries in these systems.[12,13]

In this investigation high-voltage ZnO-based varistor ceramics doped with Al_2O_3 were prepared. The amounts of added Al_2O_3 were chosen based on previous reports in order to observe the donor effect. The influence of Al^{3+} doping in the range from a few ppm up to several thousand ppm on the microstructure development and grain growth, and the current–voltage characteristics of varistor ceramics, was analysed. It showed that additions of Al_2O_3 in the range up to a few hundred ppm are optimal, and that they significantly and specifically influence the threshold voltage, the nonlinear coefficient and the leakage current of the varistor. Also, some additional questions about the influence of Al_2O_3 on the ZnO grain growth are raised and discussed, and a mechanism for grain growth inhibition in the complex system of varistor ceramics doped with very small amounts of Al_2O_3 is proposed.

2. Experimental

ZnO-Bi_2O_3-based varistor samples with the nominal composition 95 mol% ZnO + (0.90 mol% Bi_2O_3; 1.75 mol%Sb_2O_3; 0.60 mol%Co_3O_4; 0.15 mol%Mn_3O_4; 0.80 mol% NiO; 0.80 mol% Cr_2O_3), Sb_2O_3/Bi_2O_3 ratio 1.95, doped with various amounts of Al^{3+} in the range from 0 to 5000 ppm (weight fractions) – 0 to 0.83 mol% of Al_2O_3 (Table 1) – were prepared with a conventional ceramic procedure. Reagent-grade oxides were mixed in the proper ratios and homogenised in absolute ethanol media in a polyethylene bowl with zirconia balls for 1 h at 200 rpm using a planetary mill. Al was added prior to the homogenisation in the mill as an aqueous solution of $Al(NO_3)_3{\cdot}9H_2O$ – it decomposes at about 200 °C into Al_2O_3. The powders were then dried and pressed at 200 MPa into discs with a diameter of 10 mm and a thickness of 1.5 mm. The pellets were fired at a temperature of 1200 °C for 2 h in air with a heating and cooling rate of 5 °C/min.

Table 1
Composition of the varistor samples with regard to the amount of added Al^{3+} (Al_2O_3)

Al^{3+} (ppm)	Al_2O_3 (mol%)
0	0.0000
50	0.0084
100	0.0167
175	0.0292
250	0.0418
350	0.0585
500	0.0835
700	0.1169
1000	0.1669
2000	0.3332
5000	0.8287

The microstructures of the samples were examined in backscattered-electron (BE) mode using a scanning electron microscope (SEM) JEOL JSM-5800 equiped with secondary-electron (SE) and backscattered-electron (BE) detectors for the image acquisition, and with an energy-dispersive X-ray spectrometer (EDXS) and a Link ISIS 300 Oxford Instruments analytical system. The phase compositions of the samples and the compositions of the individual phases were determined with the energy-dispersive X-ray spectroscopy (EDXS) under the following experimental conditions: accelerating voltage 20 kV, working distance 10 mm, and acquisition time 100 s. Several grains of the $Zn_7Sb_2O_{12}$ spinel-type phase were analysed per sample using the EDXS method in order to estimate the amount of the varistor dopants – oxides of Co, Mn, Ni, Cr and also Al – that were incorporated into the sample. In the samples doped with 350 ppm of Al and 700 ppm of Al the exact composition of the ZnO grains was determined for the amount of Co, Mn, Ni and Al dopants using electron-probe microanalysis (EPMA). As for the SEM analysis, polished cross-sections of the samples were carbon-coated to prevent charging and analysed in a JEOL 8600 Superprobe. The EPMA was performed at 20 kV and a probe current of 100 nA to ensure good analytical sensitivity and low detectability limits for the analysed dopants. Two wavelength-dispersive (WD) spectrometers with LiF (lithium fluoride) crystals were used for the analysis of the spectral lines, one for ZnKα and CoKα, and the other for MnKα and NiKα, while a WD spectrometer with TAP (thalium acid phthalate) was used for the analysis of the AlKα line. Eleven ZnO grains were analysed in the sample doped with 350 ppm of Al, and within each grain two point-beam analyses were performed. In the sample doped with 750 ppm of Al six grains were analysed: three points were analysed within each grain and each point was analysed three times. At each point the acquisition times were 20 s

for Zn, 100 s for Co, Mn and Ni, and 200 s for Al. Metallic Zn, Co, Mn and Ni, and mono-crystal Al_2O_3 (sapphire), were used as standards to quantify the composition of the analysed grains. The analytical data were quantified by a ZAF matrix-correction procedure.

The average ZnO grain size (D) and the grain size distribution were determined for each sample from the BE images by measuring 400 to 1400 grains/sample. The surface of each grain was measured and the grain size was determined for a circular geometry as the diameter of a circle having the same surface area as the grain.

The specimens for the transmission electron microscopy (TEM) experiments were prepared according to a standard procedure by cutting 3 mm discs from the sintered pellets, thinning and polishing to a 100 μm thickness, dimpling to 20 μm in the dimple-centre, and finally ion-milling using 4 kV Ar^+ ions (RES 010, Bal-Tec AG, Balzers, Liechtenstein) to perforation. The TEM samples were investigated using a 200-kV ultra-high-resolution field-emission gun (FEG) transmission electron microscope (JEM 2010-UHR, Jeol, Japan) equipped with a Si(Li) EDS detector fitted into an atmospheric thin-window EDS spectrometer (Model Link ISIS 300, Oxford Instruments, England).

For the DC current–voltage (I–V) characterization, silver electrodes were painted on both surfaces of the disc and fired at 600 °C in air. The nominal varistor voltages (V_N) (break-down voltage = voltage at which the varistor switches from a highly resistive to a highly conductive state) at 1 and 10 mA were measured and the threshold voltage V_T (V/mm) (break-down voltage per unit thickness of varistor ceramic; $V_T = V_N(1\,mA)/d$; d is the thickness of the sample in mm) and nonlinear coefficient α ($\alpha = \log(I_{10mA}/I_{1mA})/(\log(V_2/V_1) = 1/(\log(V_2/V_1)$ according to the equation describing I–V nonlinearity of the varistor ceramics $I = KV^{\alpha}$; K is a material constant) were determined. The leakage current (I_L) (current through the varistor in the pre-break-down region of the I–V characteristic) was measured at 0.75 V_N(1 mA).

3. Results and discussion

The microstructural and current–voltage (I–V) characterization indicated that doping with Al_2O_3, even with very low amounts added to the starting composition, strongly influenced the grain size (D) and the nonlinear characteristics of the varistor ceramics. Microstructures of the sample without added Al_2O_3 and the samples doped with various amounts of Al_2O_3 are given in Fig. 1. While the phase composition is similar for the sample without Al_2O_3 and the samples doped with Al_2O_3, a decreasing ZnO grain size with increasing amounts of Al_2O_3 added to the samples is clearly evident. Samples without added Al_2O_3 have an average ZnO grain size of about 7.5 μm. Even an addition of 100 ppm of Al^{3+} (0.0167 mol% Al_2O_3) resulted in a much smaller average ZnO grain size, of about 5.9 μm. The ZnO grain size decreased with increasing amounts of Al^{3+} up to 700 ppm (0.1169 mol% Al_2O_3), but with further amounts of Al_2O_3 the

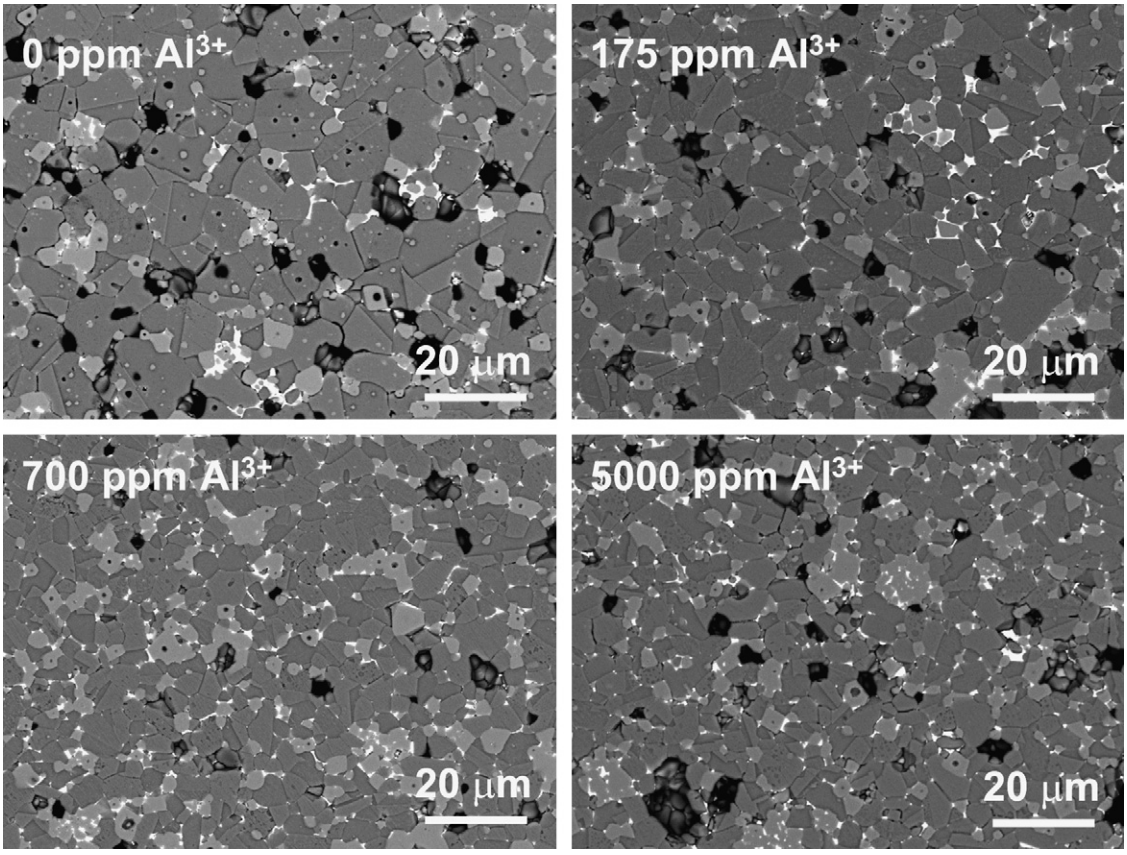

Fig. 1. Backscattered-electron (BE) images from scanning electron microscope (SEM) of microstructures of the varistor samples sintered at 1200 °C for 2 h.

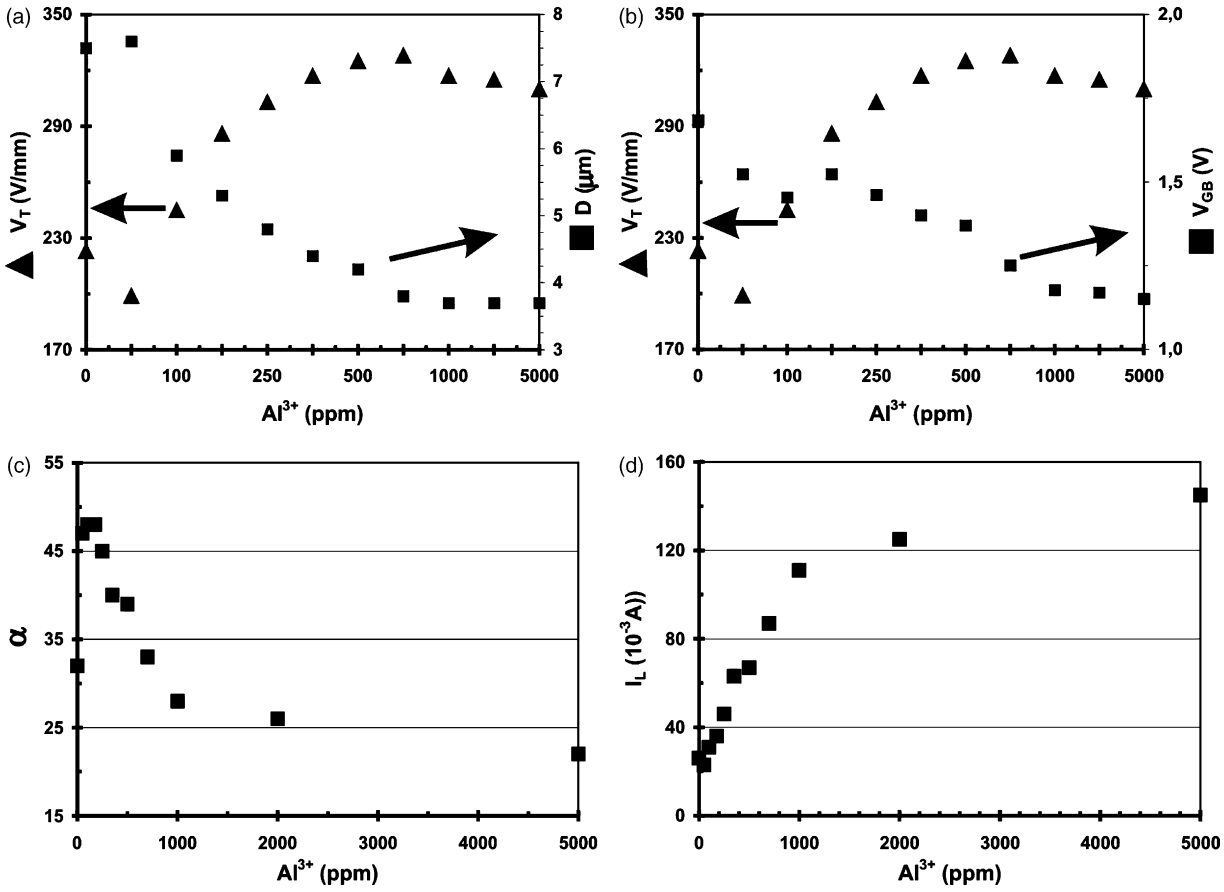

Fig. 2. Graphical presentation of the influence of the amount of added Al^{3+} to the starting composition on the (a) average ZnO grain size D and threshold voltage V_T (b) threshold voltage V_T and average break-down voltage of grain boundaries V_{GB}; (c) nonlinear coefficient α; and (d) leakage current, I_L.

grain size remained similar, at about 3.7 μm. The influence of the amount of added Al^{3+} on the average ZnO grain size of the samples sintered at 1200 °C for 2 h is graphically presented in Fig. 2a. As can be seen from the histograms in Fig. 3, doping with Al_2O_3 also strongly influenced the ZnO grain size distribution; it narrowed significantly with increasing amounts of Al_2O_3 in comparison to the Al_2O_3-free sample.

The threshold voltage, V_T, of the samples changed in accordance with the changes in the ZnO grain size – as the grain size, D, decreased, the V_T of the sample increased. The V_T steadily increased from 223 V/mm for the Al_2O_3-free sample to about 325 V/mm for the samples with 500 and 700 ppm of Al^{3+} (0.0835 and 0.1169 mol% of Al_2O_3, respectively), and for the samples with 1000 (0.1669), 2000 (0.3332) and 5000 ppm of Al^{3+} (0.8287 mol% Al_2O_3) it settled at 314 V/mm (Fig. 2b). However, according to the equation $V_T = NV_{GB} = (1/D - 1)V_{GB}$ (N is the number of grain boundaries per unit thickness of ceramic; D is the grain size in μm; and V_{GB} is the average break-down voltage of the grain boundaries), the increase of V_T is smaller than would be expected for the observed decrease in the ZnO grain size, which indicates a decrease in the V_{GB} of the Al_2O_3-doped samples. In Fig. 2b, V_{GB} versus the amount of Al^{3+} is graphically presented; it shows that even an addition of 50 ppm of Al^{3+} (0.0084 mol% Al_2O_3) resulted in a decrease in the V_{GB} in comparison to the Al_2O_3-free sample, and that the reduction in V_{GB} is most significant for additions of Al^{3+} in the range from 250 to 1000 ppm of Al^{3+} (from 0.0418 to 0.1669 mol% Al_2O_3), while in the samples doped with larger amounts of Al^{3+} the value of V_{GB} settled at 1.2 V.

The influence of the amount of Al^{3+} on the nonlinear coefficient α is graphically presented in Fig. 2c. Even an addition of 50 ppm of Al^{3+} (0.0084 mol% Al_2O_3) positively influenced the nonlinear coefficient α and raised it from 32 for the Al_2O_3-free sample to about 47 for the doped sample. The nonlinear coefficient α remained at such a level up to the addition of 250 ppm of Al^{3+} (0.0418 mol% Al_2O_3), and then steadily decreased for the larger additions of Al^{3+}, down to 22 for the sample doped with 5000 ppm of Al^{3+} (0.83 mol% Al_2O_3). In contrast, doping with Al_2O_3 had a negative effect on the break-down voltage of the grain boundaries, V_{GB}, which decreased with increasing additions (Fig. 2b), and the leakage current, I_L, which sharply increased with increasing amounts of Al_2O_3, from 26 μA for the Al_2O_3-free sample to about 111 μA for the sample with the addition of 1000 ppm of Al^{3+} (0.1669 mol% Al_2O_3), while for larger additions of Al_2O_3 the I_L increased further, albeit more moderately (Fig. 2d). These results are consistent with the previous reports in the literature. Gupta and coworker[4] and Gupta[5] reported a similar effect for Al_2O_3 doping on the high current nonlinearity of varistors; while α (0.1 mA–250 A/cm^2) increased with a low level of doping (~400 ppm Al), it decreased with the addition of 2000 ppm, and very drastically for 20,000 ppm of Al. They also observed a reduction in V_{GB} for samples with

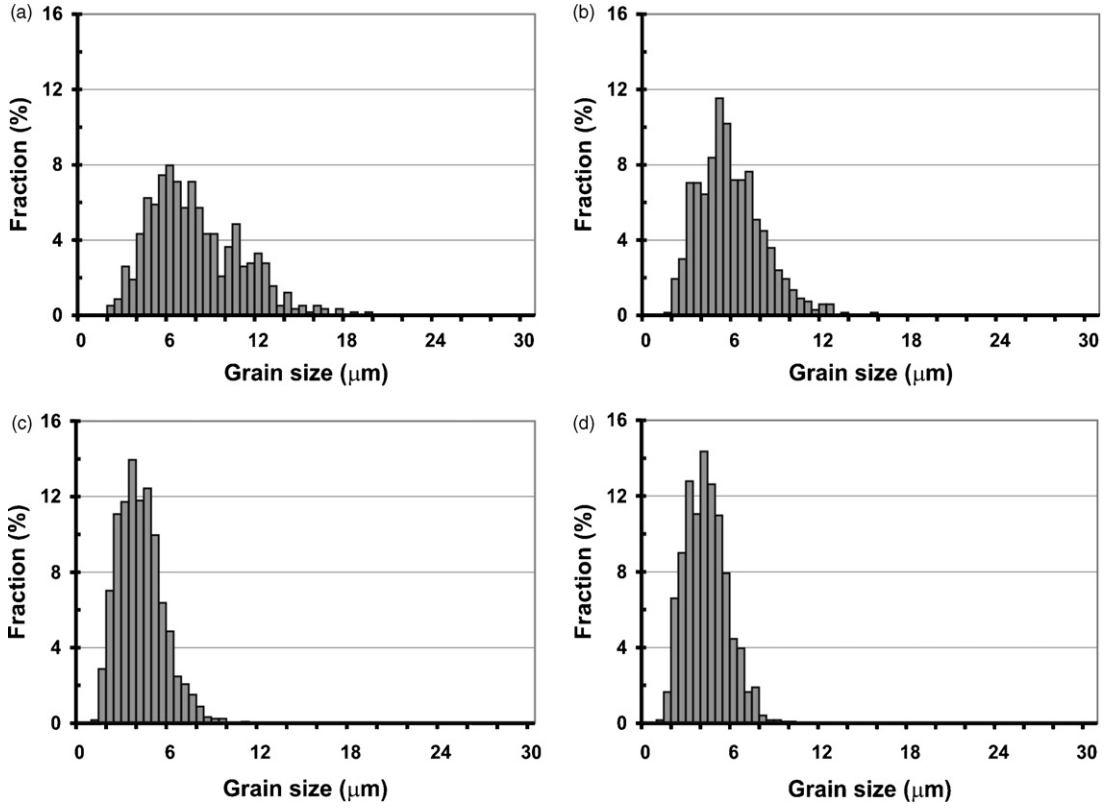

Fig. 3. Histograms of the ZnO grain size distribution of the varistor samples sintered at 1200 °C for 2 h: (a) 0 ppm Al^{3+}; (b) 175 ppm Al^{3+}; (c) 700 ppm Al^{3+}; (d) 5.000 ppm Al^{3+}.

the addition up to 500 ppm of Al. Fan and Freer[6] reported an increase of α from 38 to 60 by doping varistor samples with 500 ppm of Al. In contrast, Shouxiang et al.[9] reported a strong decrease of α: from 60 for an un-doped sample, down to 20 in the varistor samples doped with just 60 ppm of Al. In their samples they also observed a gradual rise in the leakage current with the level of Al doping. A strong increase in the leakage current in the varistor samples doped in the range from 500 to 10,000 ppm of Al was also reported by Houabes et al.[10] Such a complex and ambiguous influence of Al_2O_3 doping on the nonlinear coefficient α can be explained by the influence of Al_2O_3 on the electrical characteristics of the ZnO grains and grain boundaries. As a donor, Al^{3+} incorporates into the ZnO grains, increasing the conductivity (reducing the resistively) of the grains,[4–8,10] which can contribute to the enhanced nonlinear coefficient α of varistor ceramics. At the same time the donor effect of Al^{3+} segregated at the grain boundaries increases the concentration of the charge carriers in the grain boundary region[8,9], reduces the barrier height,[6] and decreases the resistance of the grain boundaries. This has just the opposite effect on the coefficient of nonlinearity and forces it to decrease. As long as the effect of the increased conductivity of the ZnO grains prevails, i.e., the effect of a reduced grain boundary resistance, Al_2O_3 doping results in a higher nonlinearity coefficient α while for larger amounts of Al^{3+} the nonlinearity of the varistor ceramics decays. Reduced resistivity due to the donor effect of the Al^{3+} at the grain boundaries manifests itself in an increase in the leakage current with an increasing level of Al_2O_3 doping, which can also effect the nature of the grain boundaries, indicated by a reduced average break-down voltage, V_{GB}, for the grain boundaries.

Doping with Al_2O_3 up to 0.12 mol% (~700 ppm of Al^{3+}) resulted in a significant decrease in the ZnO grain size and also in a narrower ZnO grain size distribution in comparison to the Al_2O_3-free sample (Figs. 2a and 3). Such an influence on the ZnO grain size and hence on the V_T of the varistor ceramics – as was also reported by others[4,6] – raises a question about the possible mechanism for grain growth inhibition for such small amounts of Al_2O_3 in such a complex system of varistor ceramics. The microstructural analysis showed that doping with Al_2O_3 had no influence on the phase composition of the samples. In all the samples the ZnO phase, the Bi_2O_3-rich phase and the $Zn_7Sb_2O_{12}$ spinel-type phase were observed. A typical phase composition for the samples is shown in Fig. 4. The inhibition of the ZnO grain growth in the binary ZnO-Al_2O_3 system or the ternary ZnO-Bi_2O_3-Al_2O_3 system is usually attributed to the decreased mobility of the grain boundaries caused by the pinning effect of the $ZnAl_2O_4$ spinel phase.[12,13] However, no $ZnAl_2O_4$ spinel-type phase was detected in the varistor samples analysed in this investigation, which indicated that Al_2O_3 has to influence the grain growth in some other way and that its distribution among the phases observed in the microstructure could be important. Hence, the presence of the Al_2O_3 in the secondary phases – the Bi_2O_3-rich phase and the $Zn_7Sb_2O_{12}$ spinel phase – was analysed with EDS. These phases are of micrometer and

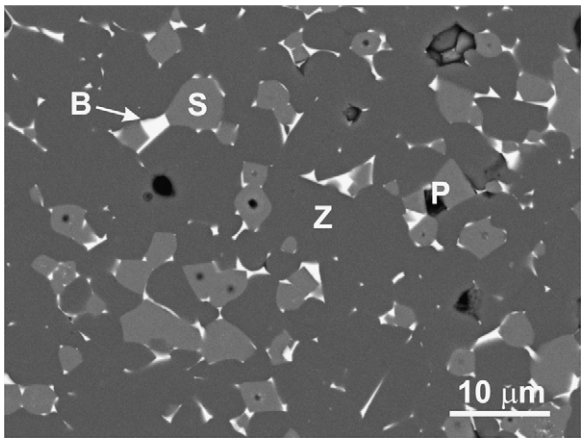

Fig. 4. Backscattered-electron (BE) image from SEM of the microstructure of the varistor sample doped with 700 ppm Al^{3+}, sintered at 1200 °C, showing typical phase composition of the samples. Z: ZnO(Co,Mn,Ni, Al) phase; B: Bi_2O_3(Zn,Co,Mn,Ni,Cr,Al)-rich phase; S: $Zn_7Sb_2O_{12}$(Co,Mn,Ni,Cr,Al) spinel-type phase; P: pore.

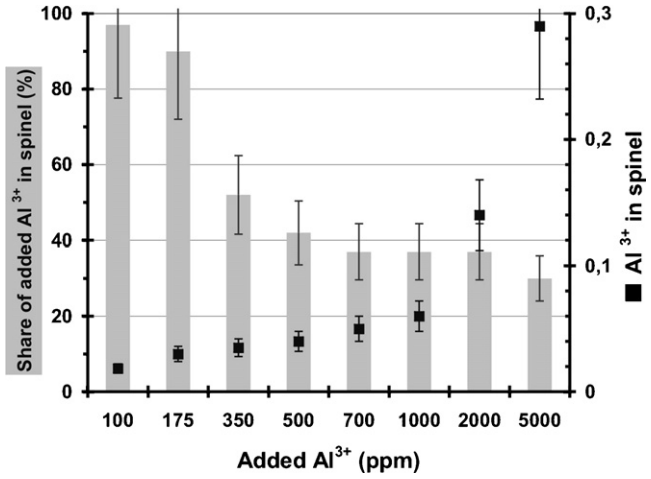

Fig. 5. Results of the EDXS analysis of Al^{3+} in the $Zn_7Sb_2O_{12}$ spinel phase.

sub-micrometer size, and due to the large probability of obtaining a signal from the neighboring phases they are not suitable for the time-demanding WDXS analysis, which has otherwise much better analytical accuracy, precision and a lower limit of detection than EDXS analysis. In the samples the ZnO grains are several micrometers in size, so the possibility of obtaining the signal from the neighboring phases is much lower in comparison to the secondary phases. Also, the solid solubility of the Al_2O_3 in the ZnO is very low and most probably below or just at the limit of detection for EDXS analysis. Therefore, WDXS analysis was used to determine the composition of the ZnO phase for selected samples. The EDS analysis showed the presence of the Al_2O_3 in the spinel phase of all the samples. The results of the EDS analysis of the spinel phase are presented in Table 2. These results should not be taken to imply that these are exact compositions of the spinel phase after sintering; they are presented in this way only to illustrate the similarity/differences in the composition of the spinel phase in the samples doped with various amounts of Al_2O_3.

The results showed a very similar composition for the spinel phase in all the samples (see average composition), and that the amount of Al_2O_3 in the spinel phase is larger in samples with larger amounts of Al^{3+} added to the starting composition. All the samples had the same starting composition for the amount of added Sb_2O_3; therefore, it is reasonable to assume that in all the samples, more or less the same amount of spinel phase is present. Based on the composition of the spinel phase and the amount of Al in it, a share of all the Al added to the starting composition that incorporated into the spinel phase was calculated. This showed that while the amount of Al in the spinel phase increases with increasing amounts of added Al, the share of all the Al^{3+} that is incorporated into the spinel phase decreases with increasing amounts of added Al^{3+}. The results are graphically presented in Fig. 5. While in the samples with additions of 100 and 175 ppm of Al^{3+} almost the entire added Al is incorporated into the spinel phase, its share in the spinel phase in samples with the addition of 500 ppm and more decreased to about 35%. With increasing amounts of Al^{3+} added to the starting composition more Al_2O_3 is present outside the spinel phase and can distribute elsewhere in the microstructure of the varistor ceramics; it can incorporate either into the ZnO grains or Bi_2O_3-rich phase, or it can also

Table 2
Average compositions of the spinel phase in the Al-doped samples determined by the EDXS analyses and normalized to nine cations, according to the formula $Zn_7Sb_2O_{12}$

Al^{3+} (ppm)	Zn (±5%)*	Sb (±10%)*	Cr (±23%)*	Mn (±20%)*	Co (±12%)*	Ni (±11%)*	Al (±60%)*	Al/Sb
0	5.97	1.63	0.61	0.21	0.23	0.35	**0.00**	–
100	5.87	1.58	0.70	0.15	0.30	0.35	**0.02**	0.0127
175	6.03	1.56	0.62	0.13	0.30	0.32	**0.03**	0.0192
250	5.88	1.60	0.70	0.13	0.31	0.33	**0.03**	0.0188
350	5.85	1.61	0.65	0.17	0.31	0.37	**0.04**	0.0248
500	5.93	1.55	0.66	0.16	0.29	0.34	**0.04**	0.0258
700	5.90	1.60	0.67	0.13	0.32	0.33	**0.05**	0.0313
1000	5.92	1.57	0.68	0.14	0.30	0.32	**0.07**	0.0446
2000	5.91	1.55	0.65	0.13	0.29	0.31	**0.14**	0.0903
5000	5.76	1.54	0.64	0.15	0.29	0.33	**0.29**	0.1883
Average ±σ (%)	5.90 (±1.2)	1.58 (±1.9)	0.66 (±4.6)	0.15 (±16.9)	0.29 (±8.4)	0.34 (±5.3)		

The amount of Al in the spinel phase increases with larger amount of Al added to the starting composition values for Al are in bold.
* Maximum standard deviation (in %) obtained in the analysis of the spinel phase from all the samples.

Table 3
Composition of the ZnO grains in varistor samples doped with 350 and 700 ppm of Al^{3+}, sintered at 1200 °C for 2 h, determined by electron-microprobe WDXS analysis

Al^{3+} (ppm)	Comp.	Zn $\pm\sigma$	Co $\pm\sigma$	Mn $\pm\sigma$	Ni $\pm\sigma$	Al $\pm\sigma$
350	Wt%	79.09 ± 0.06	0.94 ± 0.03	0.09 ± 0.01	0.19 ± 0.02	0.02 ± 0.002
	At%	98.25 ± 0.07	1.30 ± 0.04	0.13 ± 0.01	0.26 ± 0.03	0.06 ± 0.006
700	Wt%	79.12 ± 0.06	0.93 ± 0.02	0.07 ± 0.01	0.17 ± 0.02	0.05 ± 0.01
	At%	98.29 ± 0.07	1.28 ± 0.03	0.10 ± 0.01	0.24 ± 0.03	0.15 ± 0.03
$C_{DL} \geq$	Wt%	0.0140	0.0092	0.0112	0.0120	0.0025
σ_P	Wt%	0.03	0.01	0.01	0.01	0.02

C_{DL}: detectability limit by the Ziebold criterion; σ_P: precision of the analysis estimated as statistical uncertainly.

remain at the grain boundary. The EDS analysis confirmed traces of Al in the Bi_2O_3-rich phase for samples with the addition of 500 ppm of Al^{3+} (0.0835 mol% Al_2O_3) and more, while in the ZnO phase it was not detected. However, it should be noted that in the phases where Al was not detected, its presence below the limit of detection of the EDXS analysis, which is in general at about 0.1 wt%, could not be excluded.

The compositions of the ZnO phase in the samples doped with 350 and 700 ppm of Al obtained with WDXS analysis are given in Table 3. The precision of the analysis was estimated using a statistical uncertainty σ_P (wt%) for a given element, determined from the triple analysis of each point in the sample doped with 700 ppm of Al^{3+}. The compositions of the ZnO grains in both samples are similar, within the statistical uncertainty of the analysis; however, the amount of Al is appropriately higher in the grains of the sample with the larger additions of Al. In the sample with the addition of 350 ppm of Al^{3+} (0.0585 mol% Al_2O_3) about 57% of all the added Al was incorporated into the ZnO grains, while in the sample with the addition of 700 ppm (0.1169 mol% Al_2O_3) it was about 70%.

The results of the EDXS and the WDXS analyses showed that in the Al_2O_3-doped samples most of the Al was distributed between the $Zn_7Sb_2O_{12}$-type spinel phase and the ZnO phase, while only a smaller share either remained dissolved in the Bi_2O_3-rich phase or possibly segregated at the grain boundaries of the ZnO. However, this small amount of Al_2O_3 strongly influenced the current–voltage characteristics of the grain boundaries and also the grain growth in the ZnO-based varistor ceramics. Typically, in high-voltage varistor ceramics doped with Sb_2O_3, the inhibition of the ZnO grain growth is attributed to the $Zn_7Sb_2O_{12}$ spinel-type phase.[14,15] The samples analysed in this work are highly doped with Sb_2O_3 and contain a large amount of the $Zn_7Sb_2O_{12}$ spinel phase; hence, doping with such low amounts of Al_2O_3 and its incorporation into the spinel phase cannot increase the amount of $Zn_7Sb_2O_{12}$ spinel phase to a degree that would further affect the grain growth. Also, the microstructural analysis showed no influence of Al_2O_3 doping on the morphology (finer grain size) and the distribution of the spinel phase that could eventually have an impact on the grain growth. Doping with Al_2O_3 also did not produce another secondary phase like the $ZnAl_2O_4$ spinel phase, to which the inhibition of the ZnO grain growth was attributed in the ZnO-Al_2O_3 and ZnO-Bi_2O_3-Al_2O_3 systems.[12,13] Sb_2O_3 also triggers the formation of inversion boundaries (IBs) in ZnO grains, and in the Sb_2O_3-doped varistor ceramics single IBs are present in practically every ZnO grain. Our recent results showed that IBs strongly influence the microstructure development in ZnO-based ceramics.[16–18] Carlson and Gupta[4] reported for Al_2O_3-doped ZnO-based varistor ceramics that for small Al_2O_3 additions only a single twin boundary (inversion boundaries are often also called twin boundaries) appeared, whereas multiple twinning appeared in the samples containing 1 wt% Al_2O_3. However, in Al_2O_3-doped ZnO ceramics the formation of IBs was not observed, while dopants like In_2O_3 and Ga_2O_3 are known to result in multiple twins in the grains of ZnO ceramics.[19] In the microstructures of the Al_2O_3-doped samples analysed here no multiple twinning was observed; actually, only single IBs were observed, and they were present in most of the ZnO grains of all the samples, regardless of the level of the Al_2O_3 doping. If Al_2O_3 has any influence on the grain growth via inversion boundaries, from a knowledge of the mechanism of IB-induced grain growth,[16] this would only be possible if the Al_2O_3 somehow enhanced the nucleation of the IBs in the ZnO grains. In larger numbers in the early stage of sintering the grains with IBs can grow to a lesser extent at the expense of normal grains before they collide with one another, and the final microstructure contains smaller ZnO grains, all with IBs. However, most of the ZnO grains would contain IBs also in the case of fewer grains with IBs in the early stage of sintering, when they can grow to larger sizes before they collide. Hence, such an effect of Al_2O_3 on the grain growth via inversion boundaries could not be observed from the fully developed microstructure of a varistor ceramic.

With regard to the results and the consideration above it is most likely that small amounts of Al_2O_3 at the grain boundaries influence the diffusion of the ZnO and, consequently, the grain growth process. For doped Al_2O_3 Jorgensen[20] explained the decrease in the grain growth rate by assuming solute segregation at the grain boundaries, and he substantiated this by a higher microhardness in the Al_2O_3 near grain boundaries than in the bulk. Watari and Bradt[21] studied the grain growth of ZnO doped with alkali oxides (Li_2O, Na_2O, K_2O) and they proposed two grain growth inhibition mechanisms: (1) alkali oxide solute segregation to the ZnO grain boundaries creating a drag mechanism that reduces the grain boundary mobility, and (2) a reduction of the cation vacancy concentration and the occupation of interstitial sites by the alkali cations in the ZnO crystal lattice, which reduces the rate of diffusion of Zn^{2+}. In the case of Al_2O_3 doping it should be considered that the Al at the interstitial sites

acts as an acceptor and would result in a reduction of the leakage current of the Al_2O_3-doped varistor samples. In contrast, the increased leakage current observed in the Al_2O_3-doped samples results from the donor effect of Al, which is characteristic of the Al^{3+} incorporated into the regular Zn sites in the crystal lattice of the ZnO – Al^{3+} on the regular Zn sites increases the number of cation vacancies. The results are therefore not in favor of grain growth inhibition, which would result from a reduction of the Zn^{2+} mobility due to a reduction of the cation vacancy concentration and the occupation of interstitial sites by the Al cations. Tanahashi et al.[11] attributed the retardation of the grain growth in ZnO samples and ZnO-Bi_2O_3 (0.5 mol%) samples doped with Al_2O_3 in the range from 0 to 200 ppm (mol) to the formation of an aluminum compound thin film in the form of Al_2O_3 or $ZnAl_2O_4$ on the surface of the ZnO grains. Hence, grain boundaries in the varistor sample doped with 500 ppm of Al^{3+} (0.0835 mol% Al_2O_3) were examined on the transmission electron microscope (TEM) and analysed by EDXS. This TEM/EDXS analysis showed the presence of Bi at most of the examined ZnO-ZnO grain boundaries, often accompanied by Cr, and on some of the boundaries traces of Al were also present together with the Bi and Cr. A TEM image of the examined ZnO-ZnO grain boundary with the EDX spectra acquired across the grain boundary region is shown in Fig. 6. In the EDX spectra of the grain boundary peaks of Zn, Co and Mn are also present together with Bi and Al (the Cu peak is an artifact from the specimen holder). The EDXS taken at several points on the ZnO grain next to the examined grain boundary showed only Zn, Co and Mn. This indicated that in the EDXS of the grain boundary Zn, Co and Mn originated from the ZnO grain, while only Bi, Cr and Al are specific to the grain boundary. It is most likely that

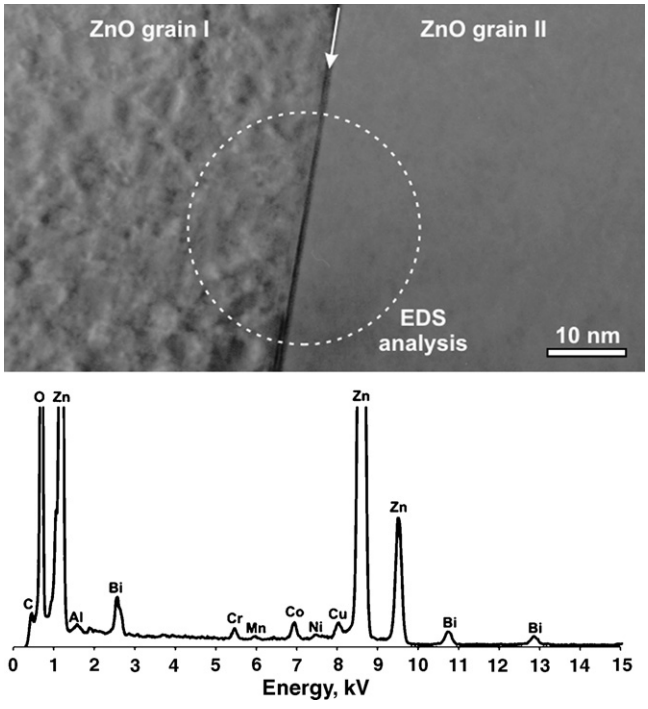

Fig. 6. TEM image of a typical grain boundary between two ZnO grains and EDS spectrum recorded across the GB region.

the detected Al is present in the Bi_2O_3 phase, as is Cr, although it cannot be completely ruled out that Al is possibly present as a thin Al_2O_3 or Zn-Al-O-type layer on the surface of the ZnO grain. On the basis of the detection of the Al_2O_3 at the grain boundaries only in the presence of the Bi_2O_3-rich phase, and also from the known chemistry of varistor ceramics, another possible mechanism for the grain growth inhibition of small amounts of Al_2O_3 in the Bi_2O_3-rich liquid phase affecting the diffusion of ZnO through the Bi_2O_3-liquid film and hence grain growth should be considered. Namely, in ZnO-based varistor ceramics grain growth takes place in the presence of the Bi_2O_3-based liquid phase. In the ZnO-Bi_2O_3 system Senda and Bradt reported[22] that at lower Bi_2O_3 levels, below 0.5 mol%, the grain growth-controlling mechanism is a solution-precipitation phase-boundary reaction of the solid ZnO and the Bi_2O_3-rich liquid phase. In this case grain growth is enhanced by a thin layer of Bi_2O_3 liquid phase at the grain boundaries of the ZnO. However, for larger amounts – about 1.0 mol% of Bi_2O_3 and more – Day and Bradt reported[23] that the grain growth rate-controlling mechanism is diffusion through the liquid phase, and the grain growth is hindered by the thickness of the Bi_2O_3 liquid layer. The samples studied in this investigation contained about 1 mol% of Bi_2O_3, and at the sintering temperature of 1200 °C the layer of Bi_2O_3-rich liquid phase in which the varistor dopants and also Al_2O_3 are dissolved is likely to be present along the majority of the grain boundaries. The possible limiting influence of small amounts of Al_2O_3 present in the Bi_2O_3-rich liquid phase on dissolving ZnO and its diffusion through the Bi_2O_3-rich liquid layer would result in hindering of the ZnO grain growth. It is well known[3] that in varistor ceramics a $Bi_3Zn_2Sb_3O_{14}$ pyrochlore-type phase is formed at temperatures as low as 600 °C. In the case of compositions with a Sb_2O_3/Bi_2O_3 ratio >1 – the samples studied in this investigation had a Sb_2O_3/Bi_2O_3 ratio of 1.95 – all the Bi_2O_3 participates in the formation of the pyrochlore phase, while the Sb_2O_3 in excess of the Bi_2O_3 at lower temperatures forms a $ZnSb_2O_6$ layer on the surface of the ZnO grains, which above 800 °C re-crystallizes into segregated grains of the $Zn_7Sb_2O_{12}$ spinel phase. It is much more likely that in such a complex system of varistor ceramics a small amount of added Al_2O_3 enters into these reactions and incorporates into pyrochlore- and Zn-Sb-O-type phases, rather than forming its own phase. At temperatures above 900 °C the pyrochlore phase decomposes into the $Zn_7Sb_2O_{12}$ spinel-type phase and the Bi_2O_3 liquid phase and the resulting Al_2O_3 is shared between these two phases. So, at the sintering temperature of the varistor samples, Al_2O_3 is present in the $Zn_7Sb_2O_7$ phase, and the Bi_2O_3-rich liquid layer spreads along the grain boundaries of the ZnO. The results of the EDXS and WDXS analyses also confirmed that: the spinel phase incorporates an appropriate amount of Al at temperatures at which the grain growth of ZnO, and hence the uptake of the Al into the ZnO grains, is still negligible. In the low-doped samples a larger part of the added Al is incorporated into the spinel phase, and only the remaining Al can incorporate into the ZnO grains during their growth. However, with an increasing amount of added Al more of it remains outside the spinel phase in the Bi_2O_3-rich liquid and can incorporate into the growing ZnO grains at the sintering temperature. On cool-

ing from the sintering temperature the excess Bi_2O_3-rich liquid phase pulls away from the ZnO-ZnO grain boundaries to the triple points, leaving behind only a thin equilibrium Bi_2O_3 layer, which produces the varistor performance of the grain boundaries. As part of this process some of the residual Al_2O_3 from the Bi_2O_3-based liquid phase and also other varistor dopants (Cr_2O_3) can stay in the Bi_2O_3 layer at the ZnO-ZnO grain boundary or segregate to the grain boundaries. However, at this stage segregated Al_2O_3 cannot effect the grain growth any more.

4. Conclusions

The influence of Al_2O_3 doping in the range 0.00–0.83 mol% (0–5000 ppm Al^{3+}) on the microstructure and current–voltage characteristics of ZnO-based varistor ceramics sintered at 1200 °C for 2 h was studied. The threshold voltage V_T (V/mm) increased with the amount of Al_2O_3 doping from 220 V for the Al_2O_3-free sample to 325 V for the sample doped with about 0.08 mol% Al_2O_3, and settled at 315 V for samples with larger additions of Al_2O_3. The nonlinear coefficient α was significantly increased by the addition of up to 0.04 mol% Al_2O_3 in comparison with the Al_2O_3-free samples, while larger additions of Al_2O_3 caused it to decrease. Doping with Al_2O_3 had a negative effect on the average break-down voltage of the grain boundaries, V_{GB}, which decreased, as well as on the leakage current, which increased sharply with additions of Al_2O_3.

Doping with Al_2O_3 strongly influenced the ZnO grain size of the samples. The average ZnO grain size of 7.5 μm for the Al_2O_3-free sample decreased to 3.8 μm with additions of Al_2O_3 up to about 0.12 mol%, while for further additions of Al_2O_3 the average grain size remained at 3.7 μm. Doping with Al_2O_3 also resulted in a greatly narrowed ZnO grain size distribution. This decrease in the ZnO grain size is mainly responsible for the significantly increased threshold voltage, V_T, of the varistor samples doped with Al_2O_3.

Doping with Al_2O_3 in the range of amounts studied in this investigation had no influence on the phase composition of the samples. In all the samples the microstructural analysis revealed the presence of the ZnO phase, the Bi_2O_3-rich phase and the $Zn_7Sb_2O_{12}$ spinel phase. No $ZnAl_2O_4$ spinel phase, to which the grain growth inhibition is attributed in the Al_2O_3-doped ZnO or ZnO-Bi_2O_3 systems according to the literature data, was detected in any of the samples. The $ZnAl_2O_4$ spinel phase can be formed in the ZnO-based varistor ceramics only with sufficiently large additions of Al_2O_3, in amounts exceeding the solubility of aluminum in the $Zn_7Sb_2O_{12}$ spinel phase, ZnO phase and Bi_2O_3-rich phase. Namely, the results of the EDXS and WDXS analyses showed that most of the Al_2O_3 added to the varistor samples distributed between the $Zn_7Sb_2O_{12}$ spinel phase and the ZnO phase, while only trace amounts were detected in the Bi_2O_3-rich phase. The spinel phase incorporates an appropriate amount of Al_2O_3 even at the low temperatures at which the grain growth of the ZnO, and hence the uptake of Al into the ZnO grains, is still negligible. The amount of Al incorporated into the spinel phase increases with increasing amounts of Al_2O_3 added to the samples, but at a lower rate. Consequently, in the low-doped samples a larger part of the added Al_2O_3 is incorporated into the spinel phase and only the remaining share can incorporate into the ZnO grains. However, with increasing amounts of added Al_2O_3 more of it remains outside the spinel phase in the Bi_2O_3-rich liquid and influences the current–voltage characteristics of the varistor samples. Only this aluminum from the Bi_2O_3-rich liquid phase can be incorporated into the growing ZnO grains at the sintering temperature. In the sample doped with about 0.06 mol% Al_2O_3 (350 ppm Al^{3+}) the ZnO grains contain about 0.02 wt% (0.06 at%) Al, while in the sample doped with about 0.12 mol% Al_2O_3 (700 ppm Al^{3+}) the ZnO grains contain 0.05 wt% (0.15 at%) of Al.

It is aluminum dissolved in the Bi_2O_3-rich phase that influences the current–voltage characteristics of the varistor ceramics; the coefficient of nonlinearity and the leakage current due to its donor effect at the grain boundaries and the break-down voltage by its influence on the grain growth, which results in a decreased ZnO grain size and a narrowed grain size distribution. The results indicate that the small amounts of Al_2O_3 present in the Bi_2O_3-rich liquid phase at the sintering temperature most likely limit the dissolving of the ZnO and its diffusion through the Bi_2O_3 liquid layer, present along most of the grain boundaries. This results in hindering of the ZnO grain growth. On cooling from the sintering temperature the excess Bi_2O_3-rich liquid phase pulls away from the ZnO-ZnO grain boundaries to the triple points, leaving behind only a thin equilibrium Bi_2O_3 layer in which traces of the Al_2O_3, and also the other varistor dopants (Cr_2O_3), can be present and effect the current–voltage characteristics of the varistor ceramics.

Acknowledgement

The authors acknowledge the financial support from the state budget by the Slovenian Research Agency (Program Contract No. P2-0084-0106/05 and Grant BI-US/04-05/30). The support of Dr. Ryna B. Marinenko from the National Institute of Standards and Technology (NIST), Chemical Science and Technology Laboratory, Surface and Microanalysis Science Division, during the quantitative electron-microprobe WDXS analysis of the varistor samples is also gratefully acknowledged.

References

1. Matsuoka, M., Nonohmic properties of zinc oxide ceramics. *Jpn. J. Appl. Phys.*, 1971, **10**, 736–746.
2. Clarke, D. R., Varistor ceramics. *J. Am. Ceram. Soc.*, 1999, **82**, 485–502.
3. Inada, M., Formation mechanism of nonohmic zinc oxide ceramics. *Jpn. J. Appl. Phys.*, 1980, **19**, 409–419.
4. Carlson, W. G. and Gupta, T. K., Improved varistor nonlinearity via donor impurity doping. *J. Appl. Phys.*, 1982, **53**, 5746–5753.
5. Gupta, T. K., Effect of minor doping on the high current application of the ZnO varistor. *Ferroelectrics*, 1990, **102**, 391–396.
6. Fan, J. and Freer, R., The roles played by Ag and Al dopants in controlling the electrical properties of ZnO varistors. *J. Appl. Phys.*, 1995, **77**, 4795–4800.
7. Han, J., Mantas, P. Q. and Senos, A. M. R., Effect of Al and Mn doping on the electrical conductivity of ZnO. *J. Eur. Ceram. Soc.*, 2001, **21**, 1883–1886.
8. Gupta, T. K., Microstructural engineering through donor and acceptor doping in the grain and grain boundary of a polycrystalline semiconducting ceramics. *J. Mater. Res.*, 1992, **7**, 3280–3295.

9. Shouxiang, H., Shiliang, W., Yuchun, X. and Xingjiao, L., Effect of aluminum doping on the electrical properties of ZnO varistors, IEEE transactions on components, hybrids, and manufacturing technology. *CHMT-8*, 1985, 525–529.
10. Houabes, M., Bernik, S. and Bui, A., The effect of aluminum oxide on the residual voltage of ZnO varistors. *Ceram. Int.*, 2005, **31**, 783–789.
11. Tanahashi, M., Ito, M., Murao, M. and Iga, A., Effect of Al-doping on the grain growth of ZnO. *Jpn. J. Appl. Phys.*, 1997, **36**, L573–L576.
12. Nunes, S. I. and Bradt, R. C., Grain Growth in ZnO-Bi_2O_3 ceramics with Al_2O_3 additions. *J. Am. Ceram. Soc.*, 1995, **78**, 2469–2475.
13. Han, J., Mantas, P. Q. and Senos, A. M. R., Densification and grain growth of Al-doped ZnO. *J. Mater. Res.*, 2001, **16**, 459–468.
14. Kim, J., Kimura, T. and Yamaguchi, T., Microstructure development in Sb_2O_3-doped ZnO. *J. Mater. Sci.*, 1989, **24**, 2581–2586.
15. Senda, T. and Bradt, R. C., Grain growth of zinc oxide during the sintering of zinc oxide-antimony oxide ceramics. *J. Am. Ceram. Soc.*, 1991, **74**, 1296–1302.
16. Daneu, N., Recnik, A., Bernik, S. and Kolar, D., Microstructural development in SnO-doped ZnO-Bi_2O_3 ceramics. *J. Am. Ceram. Soc.*, 2000, **83**, 3165–3171.
17. Daneu, N., Recnik, A. and Bernik, S., Grain growth control in Sb_2O_3-doped zinc oxide. *J. Am. Ceram. Soc.*, 2003, **86**, 1379–1384.
18. Bernik, S., Daneu, N. and Rečnik, A., Inversion boundary induced grain growth in TiO_2 or Sb_2O_3 doped ZnO-based varistor ceramics". *J. Eur. Ceram. Soc.*, 2004, **24**, 3703–3708.
19. Barf, J., Walther, T. and Mader, W., Twin Boundaries in zinc oxide with additions of gallium oxide. *Interface Sci.*, 2004, **12**, 213–226.
20. Jorgensen, P. J., Modification of sintering kinetics by solute segregation in Al_2O_3. *J. Am. Ceram. Soc.*, 1965, **48**, 207–210.
21. Watari, T. and Bradt, R. C., Grain growth of sintered ZnO with alkali oxide additions. *J. Ceram. Soc. Jpn.*, 1993, **101**, 1085–1089.
22. Senda, T. and Bradt, R. C., Grain growth in sintered ZnO and ZnO–Bi_2O_3 ceramics. *J. Am. Ceram. Soc.*, 1990, **73**, 106–114.
23. Day, D. and Bradt, R. C., Grain growth in ZnO during Bi_2O_3 liquid-phase sintering. *J. Am. Ceram. Soc.*, 1992, **75**, 2529–2534.